

## Bicarbonate Permeability of the Outwardly Rectifying Anion Channel

J.A. Tabcharani<sup>†</sup>, T.J. Jensen<sup>‡</sup>, J.R. Riordan<sup>‡</sup>, and J.W. Hanrahan<sup>†</sup>

<sup>†</sup>Department of Physiology, McGill University, Montreal, Quebec, Canada H3G 1Y6, and <sup>‡</sup>Department of Biochemistry, Hospital for Sick Children Research Institute and University of Toronto, Toronto, Ontario, Canada M5G 1X8

**Summary.** Single anion-selective channels have been studied in cultured human epithelial cells using the patch-clamp technique. Three cell types were used as models for different anion transport systems: (i) PANC-1, a cell line derived from the pancreatic duct, (ii) T<sub>84</sub>, a Cl-secreting colonic cell line, and (iii) primary cultures of sweat duct epithelium. Outwardly rectifying anion-selective channels were observed in all three preparations and were indistinguishable with respect to conductance, selectivity and gating. Striking similarities between HCO<sub>3</sub><sup>-</sup> and Cl-secreting epithelia, and the high density of outward rectifiers in pancreatic cells prompted us to study HCO<sub>3</sub> permeation through this channel. HCO<sub>3</sub> permeability was significant when channels were bathed in symmetrical 150 mM HCO<sub>3</sub> solutions, Cl-HCO<sub>3</sub> mixtures, and under bi-ionic conditions with outwardly and inwardly directed HCO<sub>3</sub> gradients. Permeability ratios ( $P_{\text{HCO}_3}/P_{\text{Cl}}$ ) estimated from bi-ionic reversal potentials ranged from 0.50 to 0.64, although conductance ratios greater than 1.2 were observed with high extracellular pH. Chloride did not inhibit HCO<sub>3</sub> permeation noticeably but rather had a small stimulatory effect when present on the opposite side of the membrane. The prevalence of outward rectifiers in PANC-1 and their permeability to bicarbonate suggests the channel may have a dual role in HCO<sub>3</sub> secretion; to allow Cl recycling at the apical membrane and to mediate some of the HCO<sub>3</sub> flux. Defective modulation of this channel in cystic fibrosis might provide a common basis for dysfunction in epithelia having very different anion transport properties (e.g., HCO<sub>3</sub> secretion, Cl secretion and Cl absorption).

**Key Words** bicarbonate secretion · chloride channel · epithelia · cystic fibrosis

### Introduction

Electrogenic anion transport provides the driving force for fluid secretion across many epithelia [23]. Chloride enters epithelial cells of the airway and colon by a sodium-coupled mechanism at the basolateral membrane and exits through a conductance in the apical membrane [16, 38, 55, 57, 66]. Apical permeability determines the transepithelial Cl flux rate and is a site of regulation by second messengers such as cAMP (3'-5' cyclic adenosine monophosphate). Cl conductance has been studied at the

single-channel level and correlates with the presence of an outwardly rectifying anion channel in many epithelial preparations [2, 5, 15, 20, 22, 24, 31, 34, 65]. The outward rectifier is thought to mediate Cl secretion because its open-state probability is increased by secretagogues and because it can be activated in inside-out patches by exposure to a solution containing Mg, ATP and the catalytic subunit of cAMP-dependent protein kinase [4, 41, 56].

In epithelia of the duodenum and pancreatic duct, most fluid secretion is driven by transport of bicarbonate rather than chloride and high luminal HCO<sub>3</sub> concentrations (>140 mM) can be achieved by some tissues. Bicarbonate secretion resembles Cl secretion because it is electrogenic and stimulated by secretagogues that elevate cAMP [17, 19, 51, 52, 58, *see also* 59], however, the pathways mediating apical HCO<sub>3</sub> exit are not well established and there is evidence for electroneutral and electrogenic mechanisms. A model for HCO<sub>3</sub> secretion across turtle urinary bladder has been proposed in which HCO<sub>3</sub> exits the cells in exchange for luminal Cl and most Cl ions entering on the exchanger leak back to the lumen (along with some HCO<sub>3</sub>) through a cAMP-activated conductance [60]. Recently, this scheme has been applied to other HCO<sub>3</sub>-secreting tissues, particularly the interlobular duct of the rat pancreas [25, 46]. However, data from rat pancreatic duct are more consistent with HCO<sub>3</sub> exiting by Cl/HCO<sub>3</sub> exchange than through a conductive pathway [46] and the analogy with Cl secretion is further weakened by the recent description of a low-conductance Cl channel in rat pancreatic duct that is clearly different from the one described in Cl-secreting tissues. It has been proposed that this novel low-conductance chloride channel mediates Cl recycling at the apical membrane of pancreatic ductal cells [26].

The purpose of this study was to determine if the outwardly rectifying anion channel described in

Cl transporting epithelia is also present in human pancreatic ductal cells, and also to measure its  $\text{HCO}_3^-$  permeability under various conditions. Our results indicate that the outward rectifier is expressed at unusually high density in PANC-1, a pancreatic cell line that maintains many differentiated properties of ductal epithelium (43). Outward rectifiers from PANC-1 were indistinguishable from those in  $T_{84}$ , a Cl-secretory cell line, and in primary cultures of the reabsorptive sweat duct, a tissue with high passive Cl conductance [see 47].  $\text{HCO}_3^-$  current flowing through the outwardly rectifying channel was studied when the membrane was bathed with symmetrical  $\text{HCO}_3^-$  solutions, under bi-ionic conditions, and with mixtures of  $\text{HCO}_3^-$  and Cl. Bicarbonate permeability was significant under all conditions examined and was 50–64% that of chloride according to most protocols. Although intracellular [Cl] is several times higher than [ $\text{HCO}_3^-$ ] and the channel prefers Cl, currents carried by each anion will be proportional to their net electrochemical gradients and ionic conductances, not their intracellular concentrations. If the outward electrochemical gradient for Cl declines during secretagogue activation as a result of Cl efflux and membrane depolarization [46], the fraction of anion current carried by  $\text{HCO}_3^-$  during steady-state stimulation may be significant.

## Materials and Methods

### CELLS

PANC-1 cells and  $T_{84}$  cells were obtained from American Type Culture Collection (Rockville, MD) and studied during the first 100 passages. Cells were plated on glass coverslips at a density of 400,000/cm<sup>2</sup>. PANC-1 cells were maintained in Dulbecco's modified Eagle's medium supplemented with 10% fetal bovine serum (FBS), penicillin (100 U/ml) and streptomycin (100 µg/ml).  $T_{84}$  cells were cultured in a 50:50 mixture of DMEM and F-12 media supplemented with 5% FBS, penicillin (100 U/ml) and streptomycin (100 µg/ml). Sweat ducts were isolated from skin biopsies from young adult donors and cultured as described previously [14]. Briefly, skin samples were digested for 18 hr with 1 mg/ml Type I collagenase dissolved in alpha MEM medium containing 1% fetal bovine serum. After excising and uncoiling individual sweat glands from the remaining epidermis, the ductal portion was transferred along with a few µl of solution to the surface of a glass coverslip coated with Cell-Tak (BioPolymers, Farmington, CT) and left overnight at 37°C in a humidified 5% CO<sub>2</sub> incubator. Medium was added on the second day and cell outgrowth followed for approximately two weeks prior to electrophysiological studies. All regulations of the Medical Research Council (Canada) and the U.S. Department of Health and Human Services concerning procurement and use of human tissues were followed.

### SOLUTIONS

Cells were transferred to a recording chamber containing a simple NaCl solution (meq/liter): 150 Na, 154 Cl, 2 Ca, 10 HEPES, 1 ethylene glycol-bis(beta-aminoethyl ether) N,N,N',N'-tetraacetic acid (EGTA), pH 7.4; or "normal bathing saline" (NBS): 154 Cl, 140 Na, 4 K, 2 Mg, 4 Ca, 10 N-2-hydroxyethylpiperazine-N'-2-ethanesulfonic acid (HEPES), 5 glucose, pH 7.4.

We notice during preliminary experiments that 10 mM HEPES reduced channel conductance ~30%, but it was used regardless because the effect on conductance was very consistent and because flickery block was often observed using other pH buffers such as MES (2[N-Morpholino] ethanesulfonate; pK<sub>a</sub> = 6.1), MOPS (3[N-Morpholino] propanesulfonate; pK<sub>a</sub> = 7.2) and TRIS (tri-imino sulfonate, pK<sub>a</sub> = 7.8). The effect of HEPES on this channel is different from its actions on neuronal Cl channels [67] and will be detailed in a later paper. Buffer artifacts were minimized throughout the present study by comparing  $\text{HCO}_3^-$  and Cl currents under identical conditions of [HEPES] and extra- and intracellular pH. The weak buffering provided by HEPES in strongly alkaline and acidic solutions was sufficient to maintain pH constant within 0.02 units. Bicarbonate solutions were equilibrated with air or 5% CO<sub>2</sub> and then titrated to the appropriate pH. Control current-voltage relationships in symmetrical Cl were not affected by exposure of patches to CO<sub>2</sub>-containing  $\text{HCO}_3^-$  solutions (see Results). The final Cl activity of all solutions was checked using an ion-selective electrode. Experiments were carried out at 20 ± 1°C.

### ELECTRICAL RECORDING

Currents were recorded using the inside-out patches [32]. Pipettes were pulled in two stages (PP-83, Narishige Scientific Instrument Lab., Tokyo) and had resistances of 4–6 MΩ when filled with 150 mM NaCl solution. The pipette contained a chlorided Ag-AgCl wire. The bath was grounded through an agar bridge having the same ionic composition as the pipette solution. Original traces in the Results section show the applied membrane potential, but the current-voltage (*I/V*) relationships and all calculations were corrected for liquid junction potentials as described previously [33]. Liquid junction potentials estimated experimentally by this method (7.3 mV in pure 150 mM solutions) were nearly identical to those calculated from the Nernst-Planck equation and published values for Cl and  $\text{HCO}_3^-$  limiting equivalent conductivities [3, 64].

Currents were amplified using an Axopatch 1B (Axon Instruments, Foster City, CA) or Yale Mk V patch clamp and recorded on video cassette tape by a pulse coded modulation-type recording adapter (DR384, NeuroData Instruments, New York, NY). During playback, single-channel records were low-pass filtered using an 8-pole Bessel filter (902LPF, Frequency Devices, Haverhill, MA) set at 600 Hz (final cutoff frequency 514 Hz) and sampled at 0.5- or 1.0-msec intervals by the computer's A/D converter.

### ANALYSIS

Data were analyzed and fitted using a laboratory microcomputer (Indec Systems, Sunnyvale, CA). Current-voltage relationships were calculated by a semi-automated procedure that involved

computing amplitude histograms for short segments of record and displaying them on a split screen next to the raw data so that current transitions and peaks could be verified using cursors. At least ten open events were measured at each steady-state potential, averaged, and entered into an  $I/V$  curve that was displayed at the end of the run to avoid bias. Slope conductance was determined by linear regression over the voltage ranges specified in the Results section. The zero current potential ( $E_{rev}$ ) was obtained by interpolation after fitting the entire  $I/V$  curve with a fourth-degree polynomial, except when currents were recorded with 30 mM salt solutions, in which case curves had to be fitted with third-degree polynomials and extrapolated to  $E_{rev}$ . Relative  $\text{HCO}_3^-$  permeability was calculated from the shift in  $E_{rev}$  [36] after substituting  $\text{HCO}_3^-$  for Cl. For example, when  $\text{HCO}_3^-$  was substituted on the intracellular side,

$$P_{\text{HCO}_3^-}/P_{\text{Cl}} = \frac{(\text{Cl})_i}{(\text{HCO}_3^-)_i} \exp[(E_{\text{HCO}_3^-} - E_{\text{Cl}})F/RT]$$

where  $P_{\text{HCO}_3^-}/P_{\text{Cl}}$  is the permeability ratio at zero net current,  $(\text{Cl})_i$  and  $(\text{HCO}_3^-)_i$  are Cl and  $\text{HCO}_3^-$  activities bathing the intracellular surface of the patch, respectively;  $E_{\text{HCO}_3^-}$  and  $E_{\text{Cl}}$  are the reversal potentials measured with  $\text{HCO}_3^-$  and Cl in the bath, respectively, and  $F$ ,  $R$ , and  $T$  have their usual meanings. This method was adequate because the channel is highly anion-selective (cation/anion permeability ratio 0.06–0.02; see Fig. 2, and [31]). Chloride and bicarbonate have similar activity coefficients (within 3% error, [7]), therefore, the same values (0.73 and 0.84 in 150 and 30 mM solutions, respectively) were used for both anions. Activities were calculated using the modified Debye-Hückel formula [49]. Significant differences were determined at the 95% confidence level using paired or unpaired Student's  $t$  tests.

## Results

### IDENTIFICATION OF THE OUTWARDLY RECTIFYING Cl CHANNEL

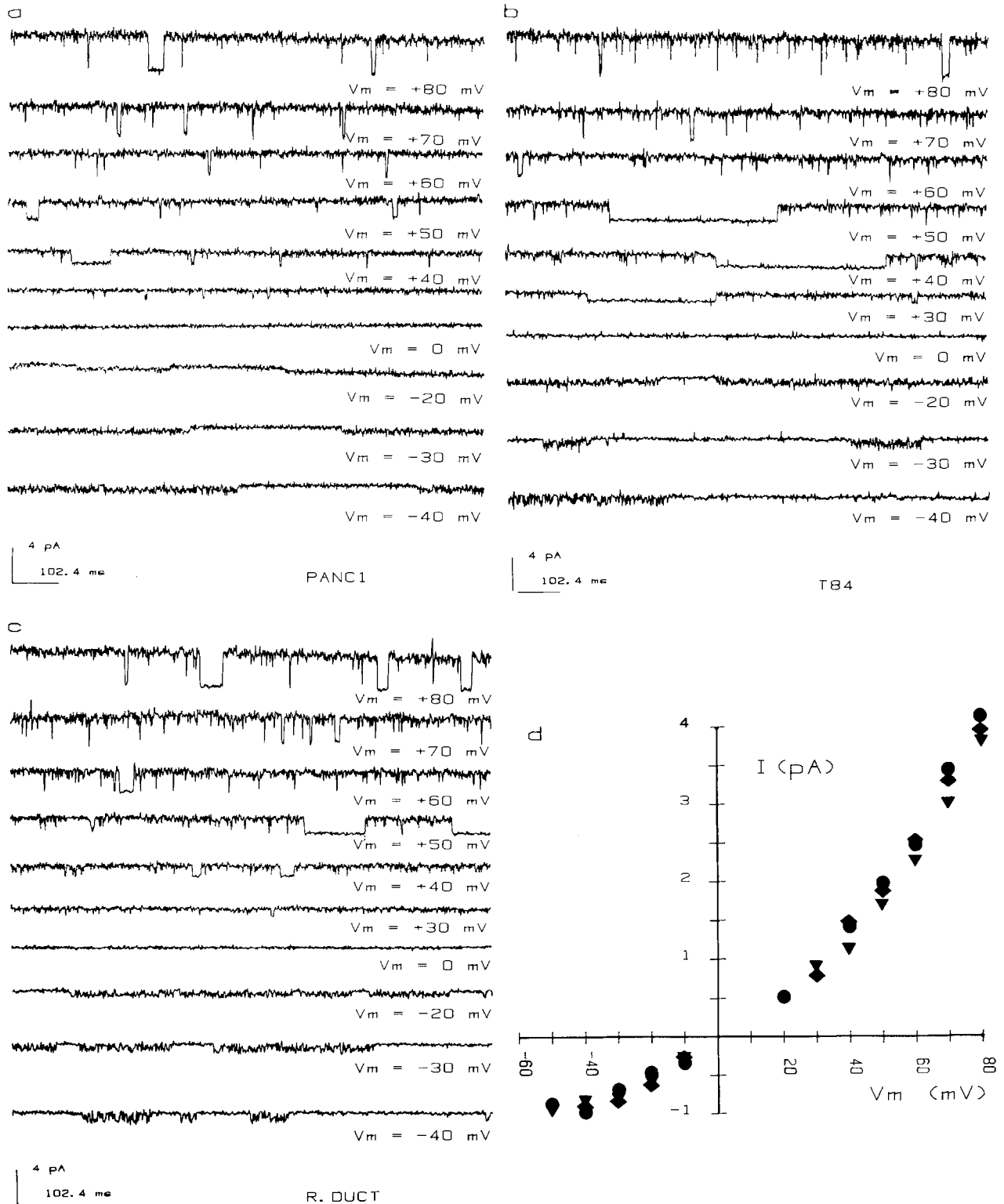
There was little spontaneous channel activity in cell-attached patches under the conditions used here. However in PANC-1 cells, Cl channels were observed in ~75% of patches that had been excised and held at +60 mV for several minutes, and those patches that contained channels usually had at least two. The density in  $T_{84}$  and sweat duct cells was lower, with approximately 30% of patches containing Cl channels, and there was usually only one channel per patch. As shown below, Cl channels were distinctive and easily identified under different conditions by their outward rectification and voltage dependence.

Figure 1a–c shows single-channel records obtained from PANC-1,  $T_{84}$  and sweat duct cells when inside-out patches were bathed symmetrically with 150 mM NaCl. Traces were obtained during the first 20 sec after clamping the membrane potential. Fig-

ure 1d shows the  $I/V$  relationships computed as described in Materials and Methods. The slope conductance at the reversal potential (calculated between –20 and +20 mV) was  $30.3 \pm 0.7$  pS ( $n = 12$  patches). Rectification was very pronounced; the slope conductance for negative currents (between –20 and –30 mV) was  $22.9 \pm 1.1$  pS and for large positive currents (between +60 and +80 mV) was  $73.4 \pm 2.0$  pS.

Rectification in NaCl solutions can be accounted for using a simple rate theory model in which Cl flux is determined by a single predominant free energy barrier (Fig. 2a). The estimated mean height of the barrier under these conditions was  $5.3 \pm 0.07$  kcal/mol. The electrical distance of the barrier was estimated to be  $38 \pm 0.6\%$  of the way through the membrane field from the intracellular side and was not affected by replacing Cl with  $\text{HCO}_3^-$  (see below). This simple model accounts very well for the  $I/V$  data under these conditions, however, parameter estimates will change in HEPES-free solution and a more elaborate model will be required to explain channel saturation and the effect of chloride-thiocyanate mixtures on conductance [29, 30]. The important result is that outwardly rectifying channels from pancreatic duct,  $T_{84}$  and sweat duct cells are indistinguishable with respect to conductance, and they closely resemble Cl channels in airway cells that function abnormally in cystic fibrosis.

Figure 2b shows the effect on the  $I/V$  relationship of isosmotically replacing 50 mM bath NaCl with sucrose. The reversal potential shifted by –25.8 mV, indicating a cation/anion permeability ratio at zero net current of 0.033. This ratio was difficult to measure accurately but was similar for channels from all cell types and averaged 0.065. Gating was voltage dependent; that is, the initial open state probability ( $P_o$ ) after stepping the membrane potential from 0 mV to different test potentials increased as the test potential was made more positive. This corresponds to the increase in  $P_o$  with depolarization, which has been reported by others (see Fig. 1a and b and [21, 31, 34]). However, unlike previous studies we also observed voltage-dependent inactivation superimposed on this process: inactivation became progressively faster as the membrane potential was clamped to increasingly positive voltages (Fig. 3) and was not affected noticeably by salt concentration or by pH. In summary, the outward rectifier was present in three cells having very different anion transport systems and was easily recognized under different experimental conditions. Cl channels from the different cell types were indistin-



**Fig. 1.** Identification of the outward rectifier: single channels recorded from (a) PANC1, (b) T<sub>84</sub>, and (c) reabsorptive sweat duct cells using symmetrical solutions containing 150 mM NaCl, 10 mM HEPES (pH 7.4). Membrane voltage is shown with respect to the extracellular (pipette) solution and positive (outward) membrane current is upward. Currents are larger at positive than at negative potentials, and initial open-state probability at positive voltages is much higher. (d) Currents were indistinguishable whether channels were obtained from cells derived from (▼) PANC-1, (◆) T<sub>84</sub> or (●) reabsorptive sweat duct

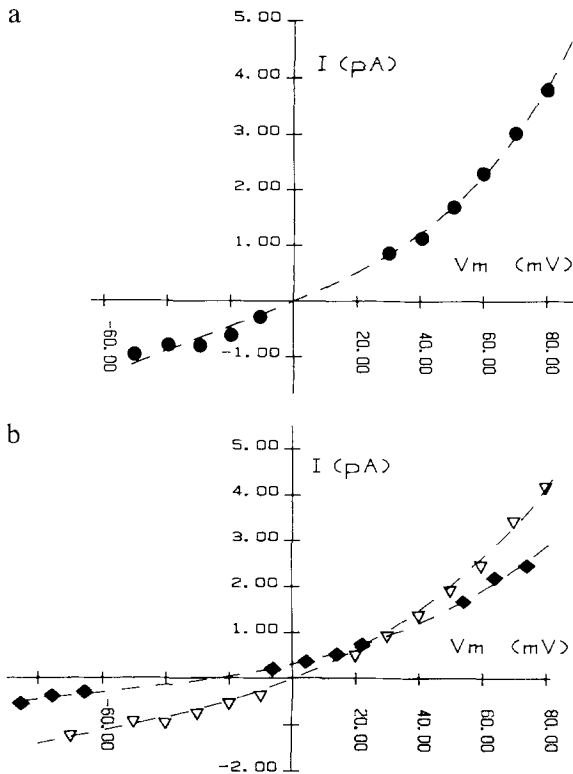
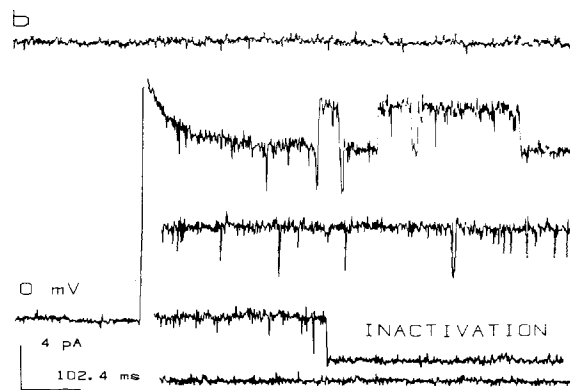
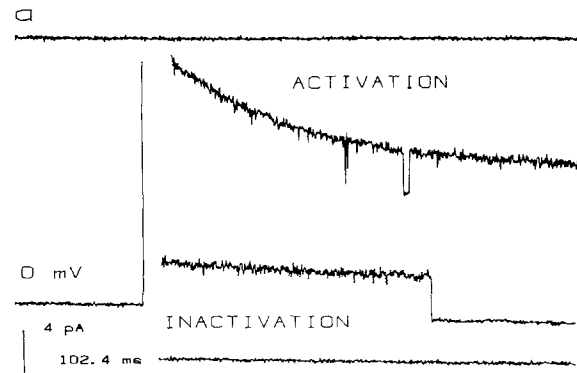


**Fig. 2.** (a) Current-voltage relationship of a channel from PANC-1 bathed symmetrically with 150 mM NaCl solution. The dashed line shows the best-fit single barrier model (height; 5.34 kcal mol<sup>-1</sup>; electrical distance from inside; 0.397). (b) Effect of reducing bath [NaCl] from (∇) 150 mM to (◆) 100 mM by replacing NaCl isosmotically with sucrose (pipette: 150 mM NaCl). Currents are shown after correcting for liquid junction potentials. The dashed lines indicate polynomial best-fits used when estimating reversal potentials. Channel was obtained from a PANC-1 cell

guishable with respect to conductance, selectivity and voltage-dependent gating. The surprisingly high density of Cl channels in the PANC-1 line suggested that this channel might mediate some HCO<sub>3</sub> efflux. Bicarbonate permeability is examined in the following sections.

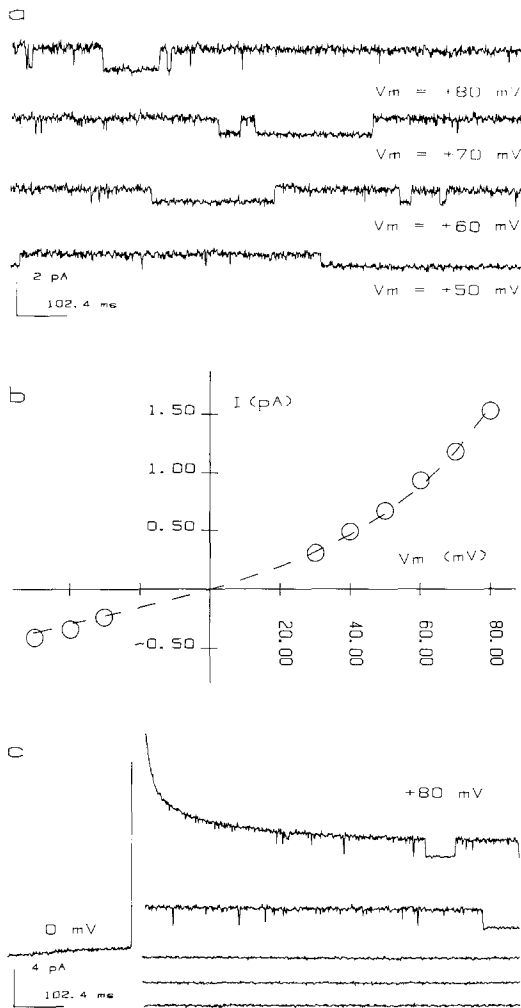
#### CONDUCTANCE IN SYMMETRICAL BICARBONATE SOLUTIONS

Figure 4a shows current traces obtained when both sides of the membrane were bathed with a solution containing nominally Cl-free, 150 mM HCO<sub>3</sub> (5% CO<sub>2</sub>, pH 8.23). Replacing Cl on both sides with HCO<sub>3</sub> did not alter the kinetics or voltage-dependent inactivation noticeably; although, currents were smaller at all potentials when carried by HCO<sub>3</sub>



**Fig. 3.** Voltage activation and inactivation of outwardly rectifying anion channels from (a) PANC-1 and (b) T<sub>84</sub> cells. Patches containing inactive channels (at +80 mV) were clamped to 0 mV for 2 sec and then back to +80 mV. The open probability was initially high after returning to +80 mV but anion channels inactivated within 2 sec at this potential. The patch in (b) contained two channels

(Fig. 4b). The slope conductance between +60 and +80 mV was  $37.0 \pm 4.5$  pS in symmetrical 150 mM HCO<sub>3</sub> solutions (mean  $\pm$  SE, five patches), about half that measured in 150 mM Cl solution (73.4 pS; see above). Negative currents were also proportionately smaller, yielding a bicarbonate conductance between -20 and -30 mV of  $10.8 \pm 1.8$  pS. At zero net current, the slope conductance was  $10.4 \pm 1.3$  pS in symmetrical HCO<sub>3</sub> solutions as compared to 29.3 pS with Cl. As shown in Fig. 4b, *I/V* curves determined in symmetrical HCO<sub>3</sub> solutions are still well-described by a simple model in which a single barrier is located  $38 \pm 0.6\%$  of the way through the membrane electric field from the intracellular side, the same electrical distance as calculated for Cl ( $P > 0.2$ ). However the barrier to HCO<sub>3</sub> permeation is significantly higher;  $5.88 \pm 0.07$  kcal/mol ( $P <$



**Fig. 4.**  $\text{HCO}_3$  permeability in symmetrical  $\text{HCO}_3$  solutions. (a) Recordings obtained with nominally Cl-free, 150 mM  $\text{NaHCO}_3$  solutions bathing both sides of the membrane. (b)  $I/V$  curve obtained with symmetrical 150  $\text{HCO}_3$ . Dashed line indicates the best-fit single barrier model (height; 5.88 kcal mol $^{-1}$ ; electrical distance from inside; 0.380). (c) Inactivation of the  $\text{HCO}_3$  current at +80 mV. Channel was obtained from a  $T_{84}$  cell

0.01). Inactivation of the  $\text{HCO}_3$  current by large positive voltage steps was identical to that observed when Cl was the charge carrier (compare Figs. 4c with 3).

#### $\text{HCO}_3$ INFLUX UNDER BI-IONIC CONDITIONS

##### *Measured with a Large pH Gradient and Small $p\text{CO}_2$ Gradient*

The concentration of NaCl and  $\text{NaHCO}_3$  solutions were reduced to 30 mM so that  $\text{HCO}_3$  flux from extra- to intracellular solution could be studied un-

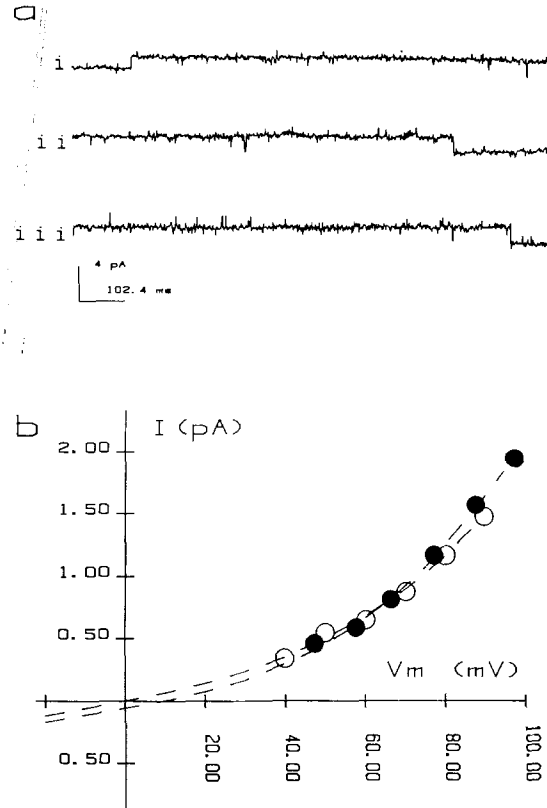


**Fig. 5.** Inward  $\text{HCO}_3$  flow with a large pH gradient and small transmembrane  $p\text{CO}_2$  gradient. (a) Single-channel currents recorded at +90 mV (i) with symmetrical 30 mM NaCl solutions (extracellular pH 9.7, 100%  $\text{N}_2$ ), and (ii, iii) with 30 mM  $\text{HCO}_3 + \text{CO}_3$  solution in the pipette (also pH 9.7, air equilibrated). Channels shown in traces i and ii were obtained from  $T_{84}$  cells; trace iii shows a channel from sweat duct. (b) Comparison of the  $I/V$  relationship obtained (○) with symmetrical 30 mM NaCl solutions or (●) with 30 mM  $\text{HCO}_3 + \text{CO}_3$  solution in the pipette. Currents carried by the inward flow of  $\text{HCO}_3 + \text{CO}_3$  (from the pipette) were larger than those carried by Cl, although extrapolated reversal potentials suggest Cl is more permeant at zero net current. Channels were obtained from reabsorptive sweat duct cells

der bi-ionic conditions without imposing a large transmembrane  $p\text{CO}_2$  gradient. Positive current, which was carried by an inward flow of anions from pipette to bath, was measured with the pipette containing 30 mM Cl solution equilibrated with  $\text{N}_2$  at pH 9.7 (the most alkaline pH at which stable patches could be maintained), or 30 mM  $\text{HCO}_3 + \text{carbonate}$  solution equilibrated with air at pH 9.7.

Figure 5a shows currents recorded at +90 mV with 30 mM Cl on both sides (trace i) and with extracellular solution containing  $\text{HCO}_3$  and carbonate ( $\text{CO}_3$ ) at the same pH (traces ii and iii). Despite channel-to-channel variation, the conductance was consistently larger with external bicarbonate when

compared with extracellular Cl, particularly at large positive voltages (Fig. 5*b*). The slope conductance calculated between +87.4 and +97.4 mV measured with external  $\text{HCO}_3^- + \text{CO}_3^{2-}$  solution was  $35.5 \pm 1.16$  pS (mean  $\pm$  SE; five patches), significantly higher than with extracellular Cl ( $31.1 \pm 0.87$  pS;  $P < 0.025$ ). However, the mean (extrapolated) reversal potential obtained with  $\text{HCO}_3^- + \text{CO}_3^{2-}$  in the pipette was  $11.1 \pm 0.9$  mV, indicating a permeability ratio  $P_{\text{HCO}_3^-}/P_{\text{Cl}} = 0.64 \pm 0.03$  (mean  $\pm$  SE, six patches). In other words, conductance ratios suggest  $\text{HCO}_3^-$  permeates as well or slightly better than chloride in the presence of a large pH gradient but reversal potentials indicate bicarbonate permeates only 64% as well. In the next section, we show that this discrepancy between conductance and permeability ratios disappears when conductance is measured with less alkaline solutions. Regardless, it is clear that the Cl channel is significantly permeable to bicarbonate and/or carbonate ions, and mediates their influx under these conditions.

#### Measured with a Large $p\text{CO}_2$ Gradient and Small pH Gradient

Inward  $\text{HCO}_3^-$  permeability was reexamined using a small transmembrane pH gradient (<1 unit) by elevating  $p\text{CO}_2$  within the pipette. The pipette was filled with a solution containing 150 mM  $\text{NaHCO}_3$  (equilibrated with 5%  $\text{CO}_2$  at pH = 8.23). Single-channel currents were measured with symmetrical 150 mM  $\text{NaHCO}_3$ , and then again after switching the bath from  $\text{NaHCO}_3$  to NaCl. A stream of humidified 5%  $\text{CO}_2$  was directed onto the bath surface whenever it contained bicarbonate.

Figure 6 shows  $I/V$  curves obtained before and after replacing bath  $\text{HCO}_3^-$  with Cl. Chloride substitution caused the reversal potential to shift from 0 mV to  $17.3 \pm 1.1$  mV (mean  $\pm$  SE; six patches), suggesting  $P_{\text{HCO}_3^-}/P_{\text{Cl}} = 0.50 \pm 0.03$ . This ratio is slightly higher than the  $\text{HCO}_3^-$ :Cl conductance ratio obtained by comparing the conductance in symmetrical Cl or  $\text{HCO}_3^-$  solutions. As explained below, this may be attributed to stimulation of conductance by Cl on the opposite side of the membrane.

#### $\text{HCO}_3^-$ EFFLUX UNDER BI-IONIC CONDITIONS

Outward bicarbonate flow (i.e., from the intra- to extracellular side of the membrane) was studied under bi-ionic conditions with 150 mM  $\text{HCO}_3^-$  in the bath. This protocol was used because rectification made it difficult to measure negative currents with air-equilibrated, 30 mM salt solutions, and because it permitted minimal carbonate ion formation. Ex-

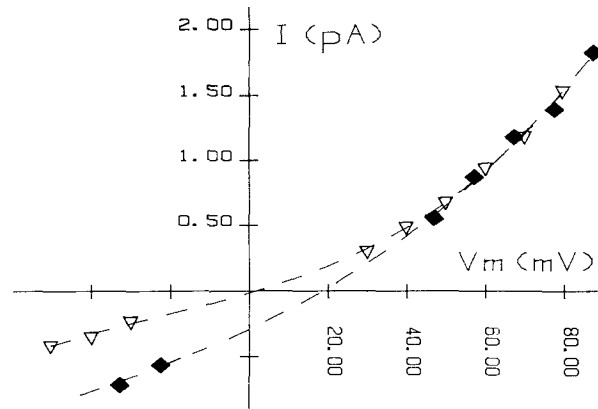
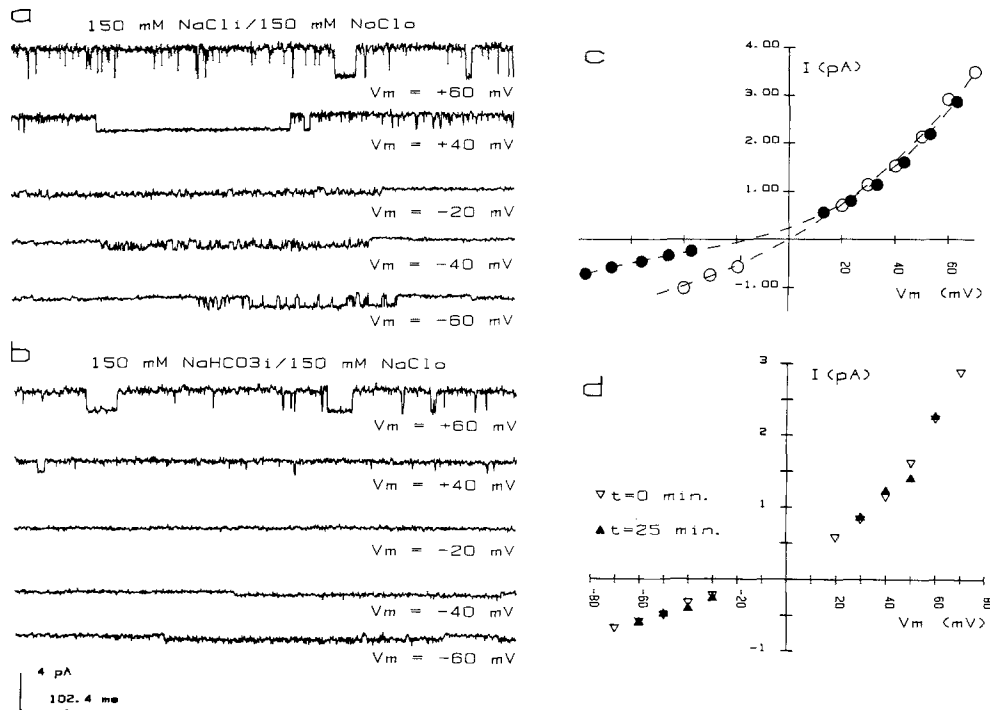


Fig. 6. Inward  $\text{HCO}_3^-$  flow with a large  $p\text{CO}_2$  gradient and small pH gradient.  $I/V$  relationships obtained ( $\nabla$ ) with symmetrical 150 mM  $\text{NaHCO}_3$  (equilibrated with 5%  $\text{CO}_2$ , pH 8.23) and ( $\blacklozenge$ ) after replacing bath  $\text{HCO}_3^-$  solution with Cl (pH 8.23, equilibrated with air). Channel was obtained from a  $T_{84}$  cell

cised patches were bathed initially by 150 mM NaCl solution (bath: pH 8.27, pipette: pH 7.3) and currents were recorded at 10–12 potentials. The bath was then flushed with 150 mM  $\text{NaHCO}_3$  solution (5%  $\text{CO}_2$ , pH 8.27) and currents were recorded again while a stream of humidified 5%  $\text{CO}_2$  was directed onto the bath surface. Measurements with  $\text{HCO}_3^-$  solutions were bracketed by control NaCl solutions (air equilibrated, pH 8.27).

Figure 7*a* and *b* shows currents recorded with symmetrical 150 mM Cl and after replacing NaCl in the bath with  $\text{NaHCO}_3$  (pH 8.23). The figure shows data obtained from a  $T_{84}$  channel but identical results were obtained when PANC-1 channels were used. Substituting  $\text{HCO}_3^-$  for Cl in the bath shifted the reversal potential by  $-15.4 \pm 0.01$  mV (mean  $\pm$  SE; five patches), indicating a  $\text{HCO}_3^-$ :Cl permeability ratio of  $0.54 \pm 0.01$  (Fig. 7*c*). Negative currents were small but were easily resolved. The  $\text{HCO}_3^-$ :Cl conductance ratio was  $0.55 \pm 0.14$  between  $-30$  and  $-50$  mV; i.e., potentials at which current would be carried by anions flowing from bath to pipette.

To determine if  $[\text{HCO}_3^-]$  in the pipette tip increased significantly during exposure of patches to  $\text{CO}_2$ ,  $I/V$  curves obtained after approximately 45-sec exposure to  $\text{CO}_2$  were compared with those obtained after 25–30 min exposure. We reasoned that if  $[\text{HCO}_3^-]$  increased significantly in the tip during this time period it should cause  $E_{\text{rev}}$  to shift in the negative direction because  $\text{HCO}_3^-$  can permeate from the extracellular side (*vide supra*). However, Fig. 7*d* shows early and late  $I/V$  curves were superimposable. Although this time interval brackets the normal duration of  $\text{CO}_2$  exposure by wide margins and used the earliest and latest times at which  $I/V$



**Fig. 7.** Outward  $\text{HCO}_3^-$  flow under bi-ionic conditions. Single channel recorded (a) with symmetrical 150 mM NaCl (pH 8.23, equilibrated with air), and (b) after replacement of bath Cl solution with  $\text{HCO}_3^-$  (pH 8.23, equilibrated with 5%  $\text{CO}_2$ ). (c)  $I/V$  relationships obtained (○) with symmetrical 150 mM NaCl and (●) after replacing the bath NaCl solution with 150 mM  $\text{NaHCO}_3$ . (d)  $I/V$  curve with symmetrical 150 mM NaCl solutions obtained immediately before (▽) and after (◆) exposure of the patch to 150 mM  $\text{HCO}_3^-$ , 5%  $\text{CO}_2$  in the bath. Channels were obtained from  $T_{84}$  cells

curves could be practically obtained, we cannot be certain  $\text{HCO}_3^-$  accumulation would be detectable within this interval. With this caveat, the results suggest the rate of  $\text{CO}_2$  diffusion into the pipette under these conditions is not sufficient to cause noticeable  $\text{HCO}_3^-$  accumulation next to the membrane.

#### BICARBONATE PERMEABILITY IN $\text{HCO}_3^-/\text{Cl}$ MIXTURES

Permeability ratios determined in pure solutions may not be physiologically applicable, as illustrated by voltage-dependent calcium channels, which are permeable to Na and K under Ca-free conditions but are highly Ca-selective in physiological salines [1, 35]. To determine if the ratio  $P_{\text{HCO}_3^-}/P_{\text{Cl}}$  is similar in the presence of Cl, outward anion flow was studied with  $\text{Cl}/\text{HCO}_3^-$  mixtures using two protocols: first,  $I/V$  curves obtained with symmetrical 150 mM  $\text{HCO}_3^-$  solutions were compared with those following replacement of 125 mM bath  $\text{HCO}_3^-$  with Cl. Second,  $I/V$  curves were compared under bi-ionic conditions (pipette: 150 mM NaCl, bath: 150 mM  $\text{NaHCO}_3$ ) and after adding 10 mM Cl to the bicarbonate solution.

Figure 8a shows traces obtained with 150  $\text{NaHCO}_3$  solution in the pipette and 125 mM NaCl + 25  $\text{NaHCO}_3$  in the bath. Changing the bath from 150 mM  $\text{NaHCO}_3$  to this mixture shifted  $E_{\text{rev}}$  from 0 mV to  $+15.0 \pm 2.47$  mV, consistent with a  $\text{HCO}_3^-/\text{Cl}$  permeability ratio of  $0.50 \pm 0.06$  (Fig. 8b; mean  $\pm$  SE, four patches). The slope conductance between  $-20$  and  $-30$  mV increased by 30%, which was expected since the current would be carried by anion flow from the bath to the pipette and Cl is more permeant. More interestingly, the slope conductance at positive voltages also increased when  $\text{HCO}_3^-$  was partially replaced by Cl; i.e., the presence of Cl in the bath enhanced  $\text{HCO}_3^-$  permeation from the opposite (extracellular) side. Figure 8c shows the effect of adding a small amount of Cl to the bath solution when it already contained 150 mM  $\text{HCO}_3^-$ . When 10 mM NaCl was added to the 150 mM  $\text{HCO}_3^-$  bath solution the reversal potential shifted from  $-15.4$  mV to  $-6.8 \pm 1.4$  mV. This corresponds to a  $\text{HCO}_3^-/\text{Cl}$  permeability ratio of  $0.70 \pm 0.04$  at zero net current, higher than the ratio obtained under bi-ionic conditions with nominally Cl-free solution in the bath ( $0.54 \pm 0.01$ ;  $P \ll 0.01$ , see above). Again the slope conductance at large de-



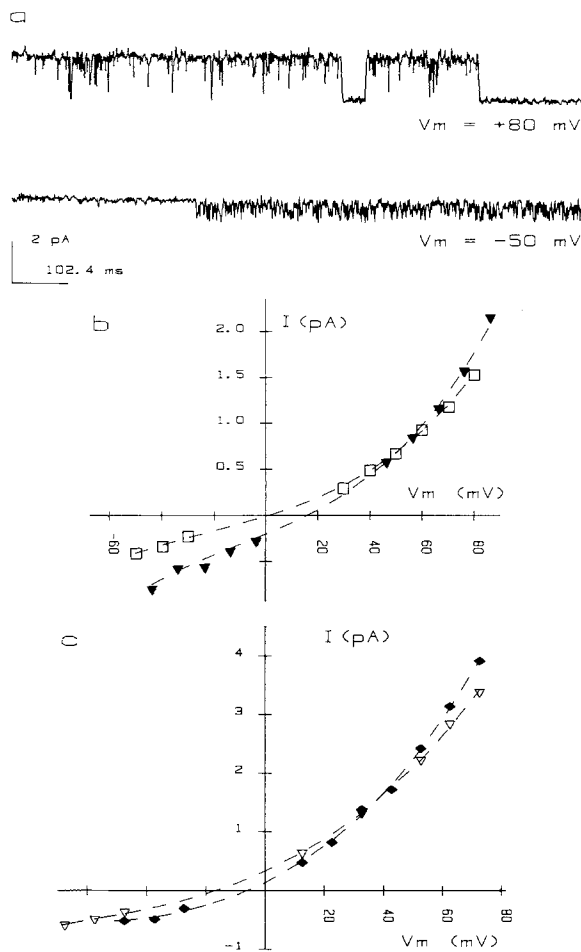


**Fig. 8.** Bicarbonate-Cl mixtures. (a) Recordings obtained with 150 mM Cl in the pipette and 125 mM Cl + 25 mM  $\text{HCO}_3^-$  in the bath (equilibrated with 5%  $\text{CO}_2$ ). (b)  $I/V$  relationships obtained ( $\square$ ) with symmetrical 150 mM  $\text{NaHCO}_3$  solutions and ( $\blacktriangledown$ ) after replacing 150 mM  $\text{NaHCO}_3$  in the bath with 125 mM NaCl + 25 mM  $\text{NaHCO}_3$ . (c)  $I/V$  relationship with 150 mM NaCl in the pipette and ( $\nabla$ ) 150 mM  $\text{NaHCO}_3$  or ( $\blacklozenge$ ) 150 mM  $\text{NaHCO}_3$  + 10 mM NaCl in the bath. Addition of low [Cl] to the bath solution enhanced anion flow from pipette to bath (i.e., in the “trans” direction) and shifted the reversal potential towards 0 mV. Channels were obtained from  $T_{84}$  cells

polarizing potentials (i.e., +60–+70 mV) was enhanced by adding Cl to the “trans” side, increasing from  $63.1 \pm 1.4$  pS when the bath contained 150 mM  $\text{HCO}_3^-$ , to  $75.0 \pm 7.62$  pS after Cl addition (mean  $\pm$  SE;  $P < 0.02$ ).

In summary, bicarbonate currents were not inhibited by the presence of Cl on either side of the membrane but were enhanced when the intracellular solution contained some Cl. This “trans-stimulation” effect may also occur in the opposite direction: the slope conductance for outward  $\text{HCO}_3^-$  flow (at  $-30$  mV) was  $22.0 \pm 1.8$  pS with Cl in the pipette

but only  $10.8 \pm 1.7$  pS when the pipette solution contained 150 mM  $\text{HCO}_3^-$  (Figs. 7 and 4).

## Discussion

Our results indicate the anion channel believed to mediate Cl transport across many epithelia is also abundant in a pancreatic cell line, PANC-1. Direct microscopic evidence that PANC-1 cells are ductal in origin was obtained by Lieber et al. using sections of the carcinoma [42]. The original tumor contained ducts lined with markedly dysplastic and malignant-type cells. More recently PANC-1 has been shown to express many differentiated properties of pancreatic ductal epithelium in vivo including: (i) epithelial intermediate filaments, (ii) basolateral localization of Na/K ATPase, (iii) formation of complete tight junctions, (iv) cuboidal ultrastructure when cells are grown on filters, (v) high levels of carbonic anhydrase, (vi) expression of gamma-glutamyltranspeptidase, and (vii) synthesis of sulfated proteins resembling those secreted by native pancreatic ducts [43].

In this study,  $\text{HCO}_3^-$  permeation through the outward rectifier was studied using several protocols. Inward bicarbonate flow was measured when the channel was bathed with  $\text{HCO}_3^-$  solution on both sides and under bi-ionic conditions in the presence of a large transmembrane pH or  $p\text{CO}_2$  gradient. Outward bicarbonate flow was determined with symmetrical  $\text{HCO}_3^-$  solutions, under bi-ionic conditions in the presence of a  $p\text{CO}_2$  gradient, and in solutions containing mixtures of  $\text{HCO}_3^-$  and Cl. Bicarbonate permeability was significant under all conditions examined.

## PROPERTIES OF THE ANION CHANNEL

Anion channels from PANC-1,  $T_{84}$  and sweat duct cells had identical  $I/V$  curves and resembled the outward rectifier described previously ( $\sim 150$  mM Cl on both sides; [5, 22, 31, 34, 65]). The slope conductances estimated at  $-30$ , 0 and  $+70$  mV (23, 30 and 73 pS, respectively) are similar to those reported for  $T_{84}$  cells (25, 41 and 71 pS, respectively; [31]), cultured airway cells (29, 30 and 62 pS; [65]; 21, 50 and 71 pS; [22]), and cultured sweat ducts (25, 38 and 80 pS; [5]). The data are also consistent with preliminary reports of outwardly rectifying anion channels in rat epididymal cells [2], *Necturus* small intestine [24] and placental trophoblast [15]. Outward rectification has been observed in another colonic cell line, HT<sub>29</sub> [34], in which  $I/V$  relationships at 37°C were well represented by two straight lines having

slopes of  $\sim 32$  and  $\sim 50$  pS at negative and positive potentials, respectively.

Channels were not usually active when patches were attached to the cell or immediately after excision, but they could be activated by large positive voltage pulses [41, 56]. Initial open-state probability at each potential increased with voltage as described previously [31, 34]. However, inactivation was also observed when the membrane potential was clamped to potentials greater than +60 mV for more than a few seconds, and the closing rate increased with positive voltage. Inactivation was removed most effectively by reversing the membrane potential. Such voltage dependence has not been reported previously in patch-clamp studies of this channel although there are preliminary reports that whole cell currents in single sweat gland cells inactivate in a similar manner [10, 44, 53]. Anion channels from rat colon incorporated into bilayers inactivate when the *cis* side of the bilayer is clamped at  $-50$  mV. This would correspond to a membrane potential of +50 mV if the channel is outwardly rectified [48]. We did not characterize voltage inactivation in detail because at present it has no obvious physiological function.

The present estimate of  $P_{\text{Cl}}/P_{\text{Na}} > 18$  is in fair agreement with earlier reports in airway (6.5; [65];  $> 10$ ; [21]), rat colon (16; [48]) and T<sub>84</sub> cells (50; [31]). Bi-ionic  $\text{HCO}_3^-:\text{Cl}$  permeability ratios ranged from 0.64 to 0.50 for  $\text{HCO}_3^-$  influx when determined at zero net current with large pH or  $p\text{CO}_2$  gradients, respectively. The permeability ratio for  $\text{HCO}_3^-$  efflux was 0.54 in the presence of a small  $p\text{CO}_2$  gradient, and 0.50 in mixed solutions containing both Cl and  $\text{HCO}_3^-$ .  $\text{HCO}_3^-:\text{Cl}$  conductance ratios varied from 0.42 for influx in the presence of a large  $p\text{CO}_2$  gradient, to 1.44 when the influx was measured with high extracellular pH. The reason for elevated conductance at high extracellular pH is not known, but it is probably a pH effect rather than carbonate ( $\text{CO}_3^{2-}$ ) conductance because sulfate, which has a smaller hydrated radius than carbonate (0.184 *vs.* 0.212 nm), was found to be only slightly permeant ( $G_{\text{SO}_4}:G_{\text{Cl}} = 0.19$ ). Carbonate permeability was not studied directly because patches became unstable at  $\text{pH} > 9.7$ . Relative permeability of the channel for bicarbonate and other anions closely resembles the transepithelial sequence measured for cat main pancreatic duct (1.9 I  $>$  1.28 Br  $>$  1 Cl  $>$  0.56  $\text{HCO}_3^-$   $>$  0.41 F [27]). This sequence was been interpreted with reference to the paracellular pathway, but a cellular component was not ruled out.

Solutions containing 150 mM  $\text{NaHCO}_3$  were equilibrated with 5%  $\text{CO}_2$ , thus a  $\text{CO}_2$  gradient favoring diffusion through the membrane was un-

avoidable when measuring selectivity under bi-ionic conditions. Membrane permeability to  $\text{CO}_2$  is relatively high, and  $\text{CO}_2$  diffusion through the lipid bilayer is not rate limiting when there is little carbonic anhydrase present [28]. Ignoring the membrane, we estimated the  $\text{CO}_2$  flux through the tip under these conditions to be  $< 1.6 \times 10^{-16}$  mol  $\text{sec}^{-1}$  using the relationship  $J = a \cdot p\text{CO}_2 \cdot D \cdot \pi \cdot \tan \theta \cdot r_1$ , where  $a$  is the solubility of  $\text{CO}_2$  in water (0.038 mol  $\text{ml}^{-1}$   $\text{atm}^{-1}$ ),  $D$  is the diffusion coefficient for  $\text{CO}_2$  ( $2 \times 10^{-5}$   $\text{cm}^2 \text{sec}^{-1}$ ),  $\theta$  is the semi-angle at the pipette tip ( $12^\circ$ ), and  $r$  is the radius of the tip opening ( $\sim 0.5$   $\mu\text{m}$ ). This calculation assumes that (i) the membrane is not a significant barrier to net  $\text{CO}_2$  flux, (ii) the  $\text{CO}_2$  flux reaches a steady state, (iii) the inside of the pipette tip is conical, and (iv) the  $p\text{CO}_2$  of the bulk solution in the pipette shank remains constant [see 40]. The diffusion coefficient for  $\text{CO}_2$  in cell membranes ( $5 \times 10^{-8}$   $\text{cm}^2 \text{sec}^{-1}$ , estimated from methanol diffusion) is lower than for  $\text{HCO}_3^-$  diffusion in water ( $\sim 10^{-5}$   $\text{cm}^2 \text{sec}^{-1}$ ), and the uncatalysed rate of  $\text{CO}_2$  hydration is relatively slow (14  $\text{sec}^{-1}$ ). Consequently,  $\text{CO}_2$  entering the pipette solution due to the  $p\text{CO}_2$  gradient would diffuse an average of 6  $\mu\text{m}$  as  $\text{CO}_2$  before conversion to  $\text{HCO}_3^-$ . These factors, combined with diffusion of  $\text{HCO}_3^-$  away from the membrane, may explain why the reversal potential was unaffected by exposure to  $\text{CO}_2$ .

The bicarbonate:Cl permeability ratio of the outward rectifier has not been measured previously using the patch-clamp technique, however, a similar value (0.4) has been reported for colonic anion channels incorporated into planar bilayers [48]. The agreement using different techniques provides further evidence that the reconstituted anion channel originates from apical vesicles and is the same one characterized in patch-clamp studies. The present results also extend the selectivity data to include conductance ratios, equilibrium permeability ratios for  $\text{HCO}_3^-$  flux in both directions, and relative  $\text{HCO}_3^-$  permeability in mixed solutions.  $\text{HCO}_3^-$  permeability is not unique to epithelial Cl channels: patch-clamp studies of neuronal GABA-activated channels yielded a  $P_{\text{HCO}_3^-}:P_{\text{Cl}}$  ratio of 0.18 [7], although recent microelectrode experiments using crayfish skeletal muscle indicate ratios of 0.46–0.53 [37].

#### IMPLICATIONS FOR $\text{HCO}_3^-$ SECRETION AND INTRACELLULAR PH

Epithelia exhibiting apical  $\text{HCO}_3^-$  conductance include duodenum, choroid plexus, turtle urinary bladder, and pancreatic duct. In frog duodenum,  $\text{HCO}_3^-$  transport occurs through an electroneutral pathway and a larger electrogenic pathway that is

activated by cAMP, prostaglandins, vasoactive intestinal peptide, cholinergic agonists and numerous other secretagogues [18]. Frog choroid plexus secretes  $\text{HCO}_3^-$  into the cerebrospinal fluid in response to beta-adrenergic agonists, cholera toxin, and other maneuvers that elevate intracellular cAMP [51]. Turtle urinary bladder secretes  $\text{HCO}_3^-$  by an electrogenic process that is Na- and Cl-independent [8], stimulated by theophylline, cAMP and IBMX [8, 52], and inhibited by the anion channel blocker anthracene-9-carboxylate [60].

A cellular model has been proposed for electrogenic  $\text{HCO}_3^-$  secretion by turtle bladder that features apical Cl/ $\text{HCO}_3^-$  exchange and anion conductance [60]. According to this scheme, apical anion conductance and Cl/ $\text{HCO}_3^-$  exchange are low in unstimulated cells. cAMP stimulates apical conductance, and the resulting fall in  $[\text{Cl}]_i$  increases the inward Cl gradient driving anion exchange. Electrodiffusive Cl exit also serves to resupply the exchanger with luminal Cl. Chloride and bicarbonate were both postulated to exit through the anion channel [24].

This model also accounts for many properties of  $\text{HCO}_3^-$  secretion across the pancreatic duct. Anion exchange is consistent with micropuncture measurements of luminal ion levels [e.g., 13, 62], the partial dependence of  $\text{HCO}_3^-$  transport on Cl [11, 50], the effects of luminal SITS on isolated, perfused ducts [46], and optical measurements of intracellular pH during Cl replacement [61]. Moreover, microelectrode data suggest the apical membrane of rat pancreatic duct cells contains anion conductance [46], and patch-clamp studies have revealed a low-conductance (4 pS) anion channel in this membrane [26]. The open probability of the 4-pS channel is increased by secretin when recorded in cell-attached patches. This channel is also present in primary cultures of human pancreatic duct, but a defect in its modulation in cystic fibrosis has not yet been demonstrated. With regard to cystic fibrosis (CF), it is tempting to speculate that outward rectifiers may also participate in pancreatic  $\text{HCO}_3^-$  secretion since a defect in cAMP regulation of this channel could provide a common biochemical basis for abnormal  $\text{HCO}_3^-$  and Cl transport in the pancreas (see [39]), and Cl transport in the airways and sweat gland where defective modulation of this channel in CF has already been demonstrated.

Several lines of evidence suggest pancreatic  $\text{HCO}_3^-$  secretion is mediated by multiple pathways. Although whole gland studies must be interpreted with caution, substantial  $\text{HCO}_3^-$  secretion can be maintained when Cl is replaced by impermeant anions [11], indicating there is a Cl-independent component. It is not clear that Cl/ $\text{HCO}_3^-$  antiport could

increase luminal  $[\text{HCO}_3^-]$  to the levels measured *in situ* when luminal  $[\text{Cl}]$  varies inversely with  $[\text{HCO}_3^-]$ . If luminal  $[\text{Cl}]$  declines from 120 mM to 20–40 mM as luminal  $[\text{HCO}_3^-]$  increases, the inward  $[\text{Cl}]$  gradient would become partially dissipated before luminal  $[\text{HCO}_3^-]$  reached its theoretical maximum value. This question of the energetics of  $\text{HCO}_3^-$  transport is most acute for species having high luminal  $\text{HCO}_3^-$  concentrations (e.g., human, >100 mM; cat, >140 mM; and pig, 160 mM). Moreover, trans-epithelial  $\text{HCO}_3^-$  and Cl gradients are partially dissipated in the main pancreatic duct of the cat and this may be mediated by Cl/ $\text{HCO}_3^-$  exchange [13, 62].

Would the channel carry significant bicarbonate flux under physiological conditions? Intracellular  $\text{HCO}_3^-$  activity is typically 10–20 mM when intracellular  $p\text{CO}_2$  approximates that of the extracellular solution and cell pH is 7.0–7.4. If applicable to the pancreatic duct, this range is four- to 10-fold higher than electrochemical equilibrium for  $\text{HCO}_3^-$  (2.5 mM) when the apical membrane potential is  $-61$  mV (perfused ducts; [46]), and two- to four-fold higher than the equilibrium value in stimulated, unperfused ducts ( $-18$  mV; [26]). Channel activation would clearly lead to some  $\text{HCO}_3^-$  efflux, although most current would initially be carried by chloride because it is also above electrochemical equilibrium and its concentration and conductivity in the channel are higher. However, during steady-state stimulation, the relative contribution of bicarbonate to anion current flowing through the apical membrane may increase because the net electrochemical gradient favoring Cl exit would decline as  $[\text{Cl}]_i$  falls and the apical membrane depolarizes [46]. It is the net electrochemical gradients (and ion conductivities) that will determine the relative magnitudes of Cl and  $\text{HCO}_3^-$  currents, not their intracellular concentrations *per se*. Assuming reasonable values for intracellular and luminal  $[\text{Cl}]$  and  $[\text{HCO}_3^-]$ , we estimate that  $\text{HCO}_3^-$  could contribute only about 18% of the apical anion conductance early in the ductal system where luminal  $[\text{Cl}]$  is high, but this value could approach 50% in the larger ducts due to the inverse relationship between luminal  $[\text{Cl}]$  and  $[\text{HCO}_3^-]$ . The rate of channel-mediated  $\text{HCO}_3^-$  efflux from particular cells *in situ* may depend on additional factors such as luminal flow rate and location along the ductal system.

Many anions partially substitute for bicarbonate in supporting fluid secretion. For example, secretion is maintained at approximately 60% of the control level in rabbit and 65% in rat pancreas when  $\text{HCO}_3^-$  is replaced by acetate [54, 63]. The apical exit step for this diverse array of anions may be an exchanger with wide substrate specificity, a collection of exchangers, or a poorly selective anion channel.

It may be relevant that the outward rectifier is permeable to many organic anions that can partially support secretion.

Activation of the anion channel would be expected to cause cell acidification if the channel mediates  $\text{HCO}_3^-$  efflux. In rabbit mandibular gland acinar cells, intracellular pH ( $\text{pH}_i$ ) falls approximately 0.2 units during acetylcholine stimulation [9]. The decline in  $\text{pH}_i$  is not sensitive to DIDS but is inhibited by the Cl channel blocker diphenylamine 2-carboxylate (DPC), suggesting  $\text{HCO}_3^-$  efflux occurs through a weakly selective anion channel [6]. Further evidence for channel-mediated  $\text{HCO}_3^-$  efflux comes from recent studies of rat parotid glands in which carbachol stimulation caused intracellular pH to fall 0.4 units when Na/H exchange was blocked by amiloride [45]. This effect was reduced by methoxolamide, a carbonic anhydrase inhibitor (e.g. [12]), and by removing exogenous  $\text{HCO}_3^-$ , but was accentuated in Cl-free medium. Carbachol-induced acidification was insensitive to the anion exchange inhibitor SITS but was inhibited by DPC. Taken together these results suggest Cl and  $\text{HCO}_3^-$  may exit via the same pathway, perhaps a calcium-activated anion channel [45]. Intracellular acidification was not observed in a recent study of pancreatic acinar cells; however, this may have been masked by Na/H exchange [6].

Relative contributions of conductive *vs.* non-conductive  $\text{HCO}_3^-$  efflux remain to be established, and will probably vary among tissues and between different species. To the extent that results from cultured cells can be extrapolated to natural epithelia, we anticipate channel-mediated  $\text{HCO}_3^-$  secretion will be most significant in branches of the ductal tree where luminal [Cl] has decreased and  $\text{HCO}_3^-$  efflux occurs against a large opposing concentration gradient. Electrogenic  $\text{HCO}_3^-$  secretion may be most pronounced in species that achieve high (>140 mM) luminal  $\text{HCO}_3^-$  concentrations. Establishing the relative importance of apical pathways will require measurements of net  $\text{HCO}_3^-$  flux and net electrochemical gradients for both anions.

We thank Drs. M. Gray (Newcastle), I. Novak (Copenhagen), and M. Sarras, Jr. (Kansas City) for stimulating discussions, and Ms. D. Elie for technical assistance. This work was supported by the U.S. and Canadian Cystic Fibrosis Foundations and by the Medical Research Council (Canada). J.W.H. is the recipient of an MRC Research Scholarship.

Preliminary reports of this work were presented to the Koninklijke Nederlandse Akademie van Wetenschappen, May 1988, and the American Physiological Society, October 1988.

## References

1. Almers, W., McClesky, E.W. 1984. The nonselective conductance in calcium channels of frog muscle: Calcium selectivity in a single-file pore. *J. Physiol. (London)* **353**:585–608
2. Ashford, M.L.J. 1986. Single channel currents in cultured rat epididymal cells. *J. Physiol. (London)* **371**:142P
3. Barry, P.H., Diamond, J.M. 1970. Junction potentials, electrode standard potentials, and other problems in interpreting electrical properties of membranes. *J. Membrane Biol.* **3**:93–122
4. Bear, C.E. 1988. Phosphorylation-activated chloride channels in human skin fibroblasts. *FEBS Lett.* **237**:145–149
5. Bijman, J., Scholte, B., De Jonge, H.R., Hoogeveen, A.T., Kansen, M., Sinaasappel, M., Kamp, A.W.M. van der. 1988. Chloride transport in cystic fibrosis: Chloride channel regulation in cultured sweat duct and cultured nasal polyp epithelium. In: Cellular and Molecular Basis of Cystic Fibrosis. pp. 133–140. G. Mastella and P.M. Quinton, editors. San Francisco Press
6. Booth, N.P., Brown, P.D., Donohue, M., Elliott, A.C., Lau, K.R., Pearce, R.J. 1988. The effects of DIDS and chloride-free solutions on the acidosis induced by acetylcholine in isolated acini from rabbit mandibular salivary gland. *J. Physiol. (London)* **403**:44P
7. Bormann, J., Hamill, O.P., Sakmann, B. 1987. Mechanism of anion permeation through channels gated by glycine and  $\gamma$ -aminobutyric acid in mouse cultured spinal neurones. *J. Physiol. (London)* **385**:243–286
8. Brodsky, W.A., Ehrensbeck, G., Durham, J. 1977. Some new aspects of anion pumping by the turtle bladder. *Acta Physiol. Scand. (Suppl.)*: 341–351
9. Brown, P.D., Dho, S., Elliott, A.C., Lau, K.R. 1988. Acetylcholine causes a transient intracellular acidosis in isolated acini from rabbit mandibular gland. *J. Physiol. (London)* **396**:171P
10. Butt, A.G., Worrell, R.T., Frizzell, R.A. 1988. A volume-sensitive epithelial chloride conductance. *FASEB J.* **2**:A1284
11. Case, R.M., Holz, J., Hutson, D., Scratcherd, T., Wynne, R.D.A. 1979. Electrolyte secretion by the isolated cat pancreas during replacement of extracellular bicarbonate by organic anions and chloride by inorganic anions. *J. Physiol. (London)* **286**:563–576
12. Case, R.M., Hunter, M., Novak, I., Young, J.A. 1984. The anionic basis of fluid secretion by the rabbit mandibular salivary gland. *J. Physiol. (London)* **349**:619–630
13. Case, R.M., Scratcherd, T. 1970. On the permeability of the pancreatic duct membrane. *Biochim. Biophys. Acta* **219**:493–495
14. Collie, G., Buchwald, M., Harper, P., Riordan, J.R. 1985. Culture of sweat gland epithelial cells from normal individuals and patients with cystic fibrosis. *In Vitro* **21**:597–602
15. Davis, B., Fisher, S., Krouse, M., Wine, J. 1988. Chloride channels in cultured human placental trophoblasts. *Pediatr. Pulmonol.* **S2**:99–100
16. Degnan, K.J., Karnaky, K.J., Zadunaisky, J.A. 1977. Active chloride transport in the in vitro opercular skin of a teleost (*Fundulus heteroclitus*), a gill-like epithelium rich in chloride cells. *J. Physiol. (London)* **271**:155–191
17. Ehrensbeck, G. 1982. Effect of 3-isobutyl-1-methylxanthine on  $\text{HCO}_3^-$  transport in turtle bladder. Evidence for electrogenic  $\text{HCO}_3^-$  secretion. *Biochim. Biophys. Acta* **684**:219–227
18. Flemstrom, G. 1987. Gastric and duodenal mucosal bicarbonate secretion. In: Physiology of the Gastrointestinal Tract. (2nd ed.) L.R. Johnson, editor. Raven, New York
19. Flemstrom, G., Heylings, J.R., Garner, A. 1982. Gastric and duodenal  $\text{HCO}_3^-$  transport in vitro: Effects of hormones and proposed local transmitters. *Am. J. Physiol.* **242**:G100–G110
20. Frizzell, R.A. 1987. Cystic fibrosis: A disease of ion channels? *Trends Neurosci.* **10**:190–193

21. Frizzell, R.A., Halm, D.R., Rechkemmer, G., Shoemaker, R.L. 1986. Chloride channel regulation in secretory epithelia. *Fed. Proc.* **45**:2727–2731
22. Frizzell, R.A., Rechkemmer, G., Shoemaker, R.L. 1986. Altered regulation of airway epithelial cell chloride channels in cystic fibrosis. *Science* **233**:558–560
23. Frizzell, R.A., Schultz, S.G. 1979. Sodium-coupled chloride transport by epithelial tissues. *Am. J. Physiol.* **236**:F1–F8
24. Giraldez, F., Sepúlveda, F.V., Sheppard, D.N. 1988. An outward rectifying Cl<sup>-</sup>-selective channel in isolated *Necturus* enterocytes. *J. Physiol. (London)* **407**:102P
25. Gray, M.A., Greenwell, J.R., Argent, B.E. 1988. Ion channels in pancreatic duct cells: Characterization and role in bicarbonate secretion. In: Cellular and Molecular Basis of Cystic Fibrosis. G. Mastella and P.M. Quinton, editors. San Francisco Press
26. Gray, M.A., Greenwell, J.R., Argent, B.E. 1988. Secretin-regulated chloride channel on the apical plasma membrane of pancreatic duct cells. *J. Membrane Biol.* **105**:131–142
27. Greenwell, J.R. 1977. The selective permeability of the pancreatic duct of the cat to monovalent ions. *Pfluegers Arch.* **367**:265–270
28. Gutknecht, J., Bisson, M.A., Tosteson, F.C. 1977. Diffusion of carbon dioxide through lipid bilayer membranes. Effects of carbonic anhydrase, bicarbonate, and unstirred layers. *J. Gen. Physiol.* **69**:779–794
29. Halm, D.R., Frizzell, R.A. 1988. Ion permeation through the apical membrane chloride channel in a secretory epithelial cell. *FASEB J.* **2**:A1283
30. Halm, D.R., Rechkemmer, G., Shoumacker, R.A., Frizzell, R.A. 1987. Biophysical properties of an apical membrane chloride channel in a secretory epithelial cell line. *Fed. Proc.* **46**:636
31. Halm, D.R., Rechkemmer, G., Shoumacker, R.A., Frizzell, R.A. 1988. Apical membrane chloride channels in a colonic cell line activated by secretory agonists. *Am. J. Physiol.* **254**:C505–C511
32. Hamill, O.P., Marty, A., Neher, E., Sakmann, B., Sigworth, F.J. 1981. Improved patch-clamp techniques for high-resolution current recording from cells and cell-free membrane patches. *Pfluegers Arch.* **391**:85–100
33. Hanrahan, J.W., Alles, W., Lewis, S.A. 1985. Single anion-selective channels in basolateral membrane of a mammalian tight epithelium. *Proc. Natl. Acad. Sci. USA* **82**:7791–7795
34. Hayslett, J.P., Gögelein, H., Kunzelmann, K., Greger, R. 1987. Characteristics of apical chloride channels in human colon cells (HT<sub>29</sub>). *Pfluegers Arch.* **410**:487–494
35. Hess, P., Tsien, R.W. 1984. Mechanism of ion permeation through calcium channels. *Nature (London)* **309**:453–456
36. Hille, B. 1973. Potassium channels in myelinated nerve: Selective permeability to small cations. *J. Gen. Physiol.* **61**:669–686
37. Kaila, K., Voipio, J. 1987. Postsynaptic fall in intracellular pH induced by GABA-activated bicarbonate conductance. *Nature (London)* **330**:163–165
38. Klyce, S.D., Wong, R.K.S. 1977. Site and mode of adrenalin action on chloride transport across the rabbit corneal epithelium. *J. Physiol. (London)* **266**:777–799
39. Kopelman, H., Corey, M., Gaskin, K., Durie, P., Weizman, Z., Forstner, G. 1988. Impaired chloride secretion, as well as bicarbonate secretion, underlies the fluid secretory defect in the cystic fibrosis pancreas. *Gastroenterology* **95**:349–355
40. Krnjević, K., Mitchell, J.F., Szerb, J.C. 1963. Determination of iontophoretic release of acetylcholine from micropipettes. *J. Physiol. (London)* **165**:421–436
41. Li, M., McCann, J.D., Liedtke, C.M., Nairn, A.C., Greengard, P., Welsh, M.J. 1988. Cyclic AMP-dependent protein kinase opens chloride channels in normal but not cystic fibrosis airway epithelium. *Nature (London)* **331**:358–360
42. Lieber, M., Mazzetta, J., Nelson-Rees, W., Kaplan, M., Todaro, G. 1975. Establishment of a continuous tumor-cell line (PANC-1) from a human carcinoma of the exocrine pancreas. *Int. J. Cancer* **15**:741–747
43. Madden, M.E., Sarras, M.P., Jr. 1988. Morphological and biochemical characterization of a human pancreatic ductal cell line (PANC-1). *Pancreas* **3**:512–528
44. McCann, J.D., Welsh, M.J., Liedtke, C.M. 1987. Chloride channel currents in normal and cystic fibrosis airway epithelial cells. *Fed. Proc.* **46**:1272 (abstr.)
45. Melvin, J.E., Moran, A., Turner, R.J. 1988. The role of HCO<sub>3</sub><sup>-</sup> and Na<sup>+</sup>/H<sup>+</sup> exchange in the response of rat parotid acinar cells to muscarinic stimulation. *J. Biol. Chem.* **263**:19564–19569
46. Novak, I., Greger, R. 1988. Properties of the luminal membrane of isolated perfused rat pancreatic ducts. Effects of cyclic AMP and blockers of chloride transport. *Pfluegers Arch.* **411**:546–553
47. Quinton, P.M. 1987. Physiology of sweat secretion. *Kidney Int.* **32**:S102–S108
48. Reinhardt, R., Bridges, R.J., Rummel, W., Lindemann, B. 1987. Properties of an anion-selective channel from rat colonic enterocyte plasma membranes reconstituted into planar phospholipid bilayers. *J. Membrane Biol.* **95**:47–54
49. Robinson, R.A., Stokes, R.H. 1965. Electrolyte Solutions. (2nd Ed.). Butterworths, London
50. Rothman, S.S., Brooks, F.P. 1965. Pancreatic secretion in vitro in “Cl-free”, “CO<sub>2</sub>-free”, and low Na<sup>+</sup> environment. *Am. J. Physiol.* **209**:790–796
51. Saito, Y., Wright, E.M. 1983. Bicarbonate transport across the frog choroid plexus and its control by cyclic nucleotides. *J. Physiol. (London)* **336**:635–648
52. Sasaki, N., Durham, J.H., Ehrenspeck, G., Brodsky, W.A. 1983. Active electrogenic mechanisms for alkali and acid transport in turtle bladders. *Am. J. Physiol.* **244**:C259–C269
53. Schoppa, N., Shorofsky, S.R., Jow, F., Fozzard, H., Nelson, D.J. 1988. Whole cell currents in cultured canine tracheal epithelial cells. *Pediatr. Pulmonol.* **S2**:101–102
54. Seow, F., Young, J.A. 1984. Anionic dependency of secretin-stimulated secretion by the isolated perfused rat pancreas. In: Secretion: Mechanism and Control. R.M. Case, J.M. Lingard, and J.A. Young, editors. pp. 97–102. Manchester University Press, Manchester
55. Shorofsky, S.R., Field, M., Fozzard, H.A. 1982. The cellular mechanism of active chloride secretion in vertebrate epithelia: Studies in intestine and trachea. *Philos. Trans. R. Soc. London* **B299**:597–607
56. Shoumacker, R.A., Shoemaker, R.L., Halm, D.R., Tallant, E.A., Wallace, R.W., Frizzell, R.A. 1987. Phosphorylation fails to activate chloride channels from cystic fibrosis airway cells. *Nature (London)* **330**:752–754
57. Silva, P., Stoff, J., Field, M., Fine, L., Forrest, J., Epstein, F.H. 1977. Mechanisms of active chloride secretion by shark rectal gland: Role of Na-K-ATPase in chloride transport. *Am. J. Physiol.* **233**:F298–F306
58. Simson, J.N.L., Merhav, A., Silen, W. 1981. Alkaline secretion by amphibian duodenum. III. Effects of dBcAMP, theophylline, and prostaglandins. *Am. J. Physiol.* **241**:G529–536

59. Smith, P.L. 1985. Electrolyte transport by alkaline gland of little skate *Raja erinacea*. *Am. J. Physiol.* **248**:R346–R352
60. Stetson, D.L., Beauwens, R., Palmisano, J., Mitchell, P.P., Steinmetz, P.R. 1985. A double-membrane model for urinary bicarbonate secretion. *Am. J. Physiol.* **249**:F546–F552
61. Stuenkel, E.L., Machen, T.E., Williams, J.A. 1988. pH regulatory mechanisms in rat pancreatic ductal cells. *Am. J. Physiol.* **254**:G925–G930
62. Swanson, C.H., Solomon, A.K. 1973. A micropuncture investigation of the whole tissue mechanism of electrolyte secretion by the in vitro rabbit pancreas. *J. Gen. Physiol.* **62**:407–429
63. Swanson, C.H., Solomon, A.K. 1975. Micropuncture analysis of the cellular mechanisms of electrolyte secretion by the in vitro rabbit pancreas. *J. Gen. Physiol.* **65**:22–45
64. Weast, R.C. (editor) 1985. CRC Handbook of Chemistry and Physics. (66th Ed.) pp. D167–D168. CRC Press, Boca Raton (FL)
65. Welsh, M.J., Leidtke, C. 1986. Chloride and potassium channels in cystic fibrosis airway epithelia. *Nature (London)* **322**:467–470
66. Welsh, M.J., Smith, P.L., Frizzell, R.A. 1983. Chloride secretion by canine tracheal epithelium: III. Membrane resistances and electromotive forces. *J. Membrane Biol.* **71**:209–218
67. Yamamoto, D., Suzuki, N. 1987. Blockage of chloride channels by HEPES buffer. *Proc. R. Soc. Lond.* **B230**:93–100

Received 27 February 1989; revised 23 May 1989